Eroding Australia: rates and processes from Bega Valley to Arnhem Land

ARJUN M. HEIMSATH[1]*, JOHN CHAPPELL[2] & KEITH FIFIELD[3]

[1]*School of Earth and Space Exploration, Arizona State University, Tempe, AZ 85287, USA*

[2]*Research School of Earth Sciences, Australian National University, Canberra, ACT 0200, Australia*

[3]*Research School of Physical Sciences and Engineering, Australian National University, Canberra, ACT 0200, Australia*

**Corresponding author (e-mail: Arjun.Heimsath@asu.edu)*

Abstract: We report erosion rates determined from *in situ* produced cosmogenic ^{10}Be across a spectrum of Australian climatic zones, from the soil-mantled SE Australian escarpment through semi-arid bedrock ranges of southern and central Australia, to soil-mantled ridges at a monsoonal tropical site near the Arnhem escarpment. Climate has a major effect on the balance between erosion and transport and also on erosion rate: the highest rates, averaging 35 m Ma^{-1}, were from soil-mantled, transport-limited spurs in the humid temperate region around the base of the SE escarpment; the lowest, averaging about 1.5 m Ma^{-1}, were from the steep, weathering-limited, rocky slopes of Kings Canyon and Mt Sonder in semi-arid central Australia. Between these extremes, other factors come into play including rock-type, slope, and recruitment of vegetation. We measured intermediate average erosion rates from rocky slopes in the semi-arid Flinders and MacDonnell ranges, and from soil-mantled sites at both semi-arid Tyler Pass in central Australia and the tropical monsoonal site. At soil-mantled sites in both the SE and tropical north, soil production generally declines exponentially with increasing soil thickness, although at the tropical site this relationship does not persist under thin soil thicknesses and the relationship here is 'humped'. Results from Tyler Pass show uniform soil thicknesses and soil production rates of about 6.5 m Ma^{-1}, supporting a longstanding hypothesis that equilibrium, soil-mantled hillslopes erode in concert with stream incision and form convex-up spurs of constant curvature. Moreover, weathering-limited slopes and spurs also occur in the same region: the average erosion rate for rocky sandstone spurs at Glen Helen is 7 m Ma^{-1}, similar to the Tyler Pass soil-mantled slopes, whereas the average rate for high, quartzite spurs at Mount Sonder is 1.8 m Ma^{-1}. The extremely low rates measured across bedrock-dominated landscapes suggest that the ridge–valley topography observed today is likely to have been shaped as long ago as the Late Miocene. These rates and processes quantified across different, undisturbed landscapes provide critical data for landscape evolution models.

It is widely held that different climatic regions are characterized by different geomorphological processes and landforms. Being a tectonically quiet continent, Australia might be expected to express, almost purely, the effect of climate on landscape evolution, modulated only by lithology and ancient structures. From the temperate eastern highlands through the monsoonal north to the arid centre, the continent presents a broad suite of climatic zones and associated landforms, ranging from soil-mantled ranges to stony mesas and inselbergs. However, the climate of Australia changed greatly during its northward drift over the last few tens of millions of years (e.g. see Fujioka & Chappell 2010), and whether the landforms seen today were formed under climates like those of today depends on their rates of geomorphological change, governed by the erosional processes acting upon them. Erosion rates determined from *in situ* cosmogenic nuclides at some sites in Australia are very low (*c*. 1 m Ma^{-1}), such as from residual hills in the semi-arid zone (Bierman & Caffee 2002). If such rates were widespread, landscapes with local relief of tens to hundreds of metres would be unlikely to have evolved under climates similar to those of today.

We explore relationships between erosion rate and geomorphological form using cosmogenic nuclide measurements of erosion rates in undisturbed hilly landscapes with local relief ranging to several hundred metres, in several climatic provinces across Australia, including the temperate SE, the monsoonal tropics and the semi-arid centre. We determined erosion rates using cosmogenic ^{10}Be and ^{26}Al in samples collected across spurs

From: BISHOP, P. & PILLANS, B. (eds) *Australian Landscapes*. Geological Society, London, Special Publications, **346**, 225–241. DOI: 10.1144/SP346.12 0305-8719/10/$15.00

and slopes, as well as average erosion rates from samples of stream and river sediments.

Concepts and methods

Landforms evolve by surface lowering, caused by loss or erosion of rock (including weathered rock). In this study, measurements of cosmogenic radionuclides (^{10}Be and ^{26}Al) are used to estimate erosion rates of both soil-mantled and bare rock surfaces [reviews of methods used here have been given by Nishiizumi *et al.* (1993), Bierman (1994), Bierman & Steig (1996), Granger *et al.* (1996), Gosse & Phillips (2001), and Cockburn & Summerfield (2004)]. As shown by Lal (1991), *in situ* cosmogenic nuclide content is inversely related to erosion rate:

$$N(z) = \frac{P_0 \mathrm{e}^{-\mu z}}{\lambda + \mu \varepsilon} \quad (1)$$

where $N(z)$ is nuclide content (atoms per gram) at depth z, P_0 is surface ($z = 0$) production rate of the nuclide of interest at the latitude and altitude of the sample site, $\mu = \rho/\Lambda$ where ρ is rock density and Λ is mean free path of cosmic rays, λ is the radionuclide decay constant, and ε is erosion rate. It is important to note that equation (1) assumes that erosion proceeds smoothly at the grain or small fragment scale and at a constant rate. Taking into account the effects of latitude, altitude and topographic shielding on P_0, equation (1) is widely used to calculate rates of erosion and soil production. The approaches to soil-mantled and rocky surfaces are, however, different, and results for both cases may be distorted by the effects of climatic shifts, and are summarized briefly.

Soil-mantled slopes. Where soil is produced through weathering of the underlying rock and soil is lost by soil transport at the same rate as it is produced, erosion equates to soil production. Where transport can be characterized as diffusion-like creep, soil thickness depends on slope curvature and, provided that factors affecting creep such as soil biota and vegetation cover remain unchanged, the balance between soil production and transport should be in steady state and soil thickness at any point should remain constant (Dietrich *et al.* 1995; Heimsath *et al.* 1997, 1999). (It should be noted that, as land surfaces are lowered, slope curvature may slowly change and steady state cannot persist indefinitely, but is approximated for metre-scale lowering where the radius of slope curvature is large relative to soil thickness.) When steady-state conditions hold, the rate of erosion/soil production can be determined from measurements of cosmogenic nuclides in weathered rock at soil base, using equation (1) with $z =$ soil thickness. One criterion for steady state is that soil depth is negative-exponentially dependent on curvature (Heimsath *et al.* 1997, 1999); another is that the rate of lowering at a point remains constant, which can be tested by measuring cosmogenic nuclide profiles down the sides of emergent bedrock tors, if present (Heimsath *et al.* 2000).

Rocky slopes. Unless rocky surfaces are eroding smoothly by solution or grain-by-grain loss, surface lowering tends to occur by intermittently shedding of joint-controlled blocks or exfoliation slabs. The apparent erosion rate calculated by equation (1) for a surface sample will vary according to the time elapsed since the surface was exposed after loss of a prior block: for example, if N_u is the nuclide content at the upper surface of a block when it falls off, the nuclide content N_b of the surface exposed immediately after it fell is

$$N_\mathrm{b} = N_\mathrm{u} \mathrm{e}^{-\mu L} \quad (2)$$

where L is block thickness. For jointed rocks with joint spacing L, the nuclide content of most surfaces should lie in the range N_b to N_u. Moreover, the mean nuclide content, $\overline{N}$, of a block at the moment of falling is

$$\overline{N} = N_\mathrm{u} \frac{(1 - \mathrm{e}^{-\mu L})}{\mu L}. \quad (3)$$

Numerical evaluation of stepwise erosion by successive block losses shows that the mean value of nuclide content in a block closely approximates the uniform-rate value in equation (1), for blocks up to several metres thick. Provided that block break-up is statistically uniform, the average content of newly fallen blocks (or sediment derived from them) will represent the average erosion rate and, having measured $\overline{N}$, the expected range of values for a set of random samples from a blocky slope can be estimated from equations (2) and (3) together (also see Reinhardt *et al.* 2007).

Effects of climatic shifts. Major climatic changes, such as occurred widely and repeatedly throughout the Quaternary Era, can nullify the assumption of uniform erosion. For example, slopes that today are soil-mantled may have had negligible soil cover under Late Pleistocene arid or periglacial conditions, in which case the cosmogenic nuclide content will be higher than expected under steady-state soil cover and the erosion rate calculated using present soil depth will be falsely low. Conversely, if slopes that today are bare rock were previously mantled by soil or sediment, the

erosion rate calculated for a bare surface will be too high. In short, where these scenarios are likely, apparent erosion rates for soil-mantled slopes should be taken as minimum estimates, and those for bare rocky surfaces as maximum estimates.

Field samples. We collected three types of sample for evaluating erosion rates: rock samples a few centimetres thick from exposed bedrock surfaces; saprolite from immediately beneath soil base in soil-mantled landforms; and sediment samples from both low-order channels and slope-foot colluvium. Only quartz-bearing rocks were sampled, from which purified quartz was prepared for measurements of ^{10}Be and ^{26}Al, following standard methods. Unless otherwise stated, cosmogenic nuclides were measured with the ANU 14UD Pelletron accelerator as described by Fifield (1999). ^{9}Be carrier blanks gave ^{10}Be $<3 \times 10^{-15}$ atoms g^{-1}, $<0.1\%$ of the concentrations in our field samples. Separate aliquots of purified quartz from the same specimen showed good reproducibility (Table 1, sample P199), and field reproducibility also was good: samples taken 1.5 m apart at a waterfall crest gave statistically equivalent results (Table 1, Br299U and Br299L), as did two samples taken 7 m apart at a low granite dome, eroding by centimetre-scale exfoliation (MD1 and MD3). Field sampling patterns varied with site, and are outlined in site descriptions, below.

Field sites

We sampled moderate to steep ranges in different Australian climatic zones, including the humid southeastern escarpment and highlands, the semi-arid Flinders Ranges in southern Australia and MacDonnell Ranges in central Australia, together with the Arnhem escarpment in the tropical monsoonal north. Those in the SE and Arnhem Land have previously been described in detail whereas results from the remainder are reported here for the first time, some of which will be the subject of later, more detailed papers. No major post-Palaeozoic orogenic movements have occurred in any of these regions, although the SE is subject to slow isostatic uplift (Lambeck & Stephenson 1985; Persano *et al.* 2002, 2005) together with late Cretaceous uplift associated with Tasman Sea rifting (Hayes & Ringis 1973). Evidence for late Cenozoic thrusting and uplift has been reported from the Flinders Ranges (Quigley *et al.* 2007*a*, *b*). However, the time and depth scales recorded by cosmogenic nuclide concentrations are small compared with long-term landscape evolution of the Australian interior, which is more fruitfully addressed by thermochronological and palaeomagnetic methods [Stewart *et al.* 1986; Belton *et al.* 2004; Pillans 2007; and see reviews by Kohn *et al.* (2002) and Vasconcelos *et al.* (2008)].

Our field sites fall into two broad groups: soil-mantled, transport-limited slopes, which were examined across all climatic zones, and bedrock-dominated, weathering-limited slopes, which were sampled only in the semi-arid ranges.

Soil-mantled sites

Southeastern Australia: Bega–Bredbo region. We summarize here results reported previously in detailed studies at two soil-mantled sites in SE NSW, one from spurs beside Nunnock River (NR) at the base of the passive-margin escarpment, inland from the town of Bega (Heimsath *et al.* 2000) and the other from Frogs Hollow (FH) on tablelands above the escarpment, *c*. 900 m above sea level (asl) (Heimsath *et al.* 2001*a*). Two further sites near NR have since been studied (see Fig. 1): one lies in lowlands *c*. 25 km SE of NR, 200 m asl ('Snug' site), and the other is a spur on the escarpment above NR that rises to the crest at

Table 1. *Repeatability tests*

Sample	Material	Prod. rate	Exp. factor	^{10}Be (10^6 atoms g^{-1})	E (m Ma^{-1})
(a) Same sample, different aliquots of quartz					
P199	Hard sandstone slope	6.89	0.95	0.22 ± 0.02	16.35 ± 1.46
P199	(repeat)	6.89	0.95	0.21 ± 0.02	17.06 ± 1.68
(b) Paired samples from same field site					
Br229U	Quartzite knickpoint	6.22	0.8	0.24 ± 0.03	11.17 ± 1.44
Br299L	Quartzite knickpoint	6.22	0.8	0.19 ± 0.02	14.07 ± 1.51
MD1	Exfoliating granite	7	1	1.56 ± 0.15	2.21 ± 0.24
MD3	Exfoliating granite	7	1	1.69 ± 0.14	2.01 ± 0.18

All errors propagated to erosion rate, E. Production factor scales nuclide prodution for slope, soil cover, elevation and latitude. Exp. factor is the correction factor applied for local exposure.

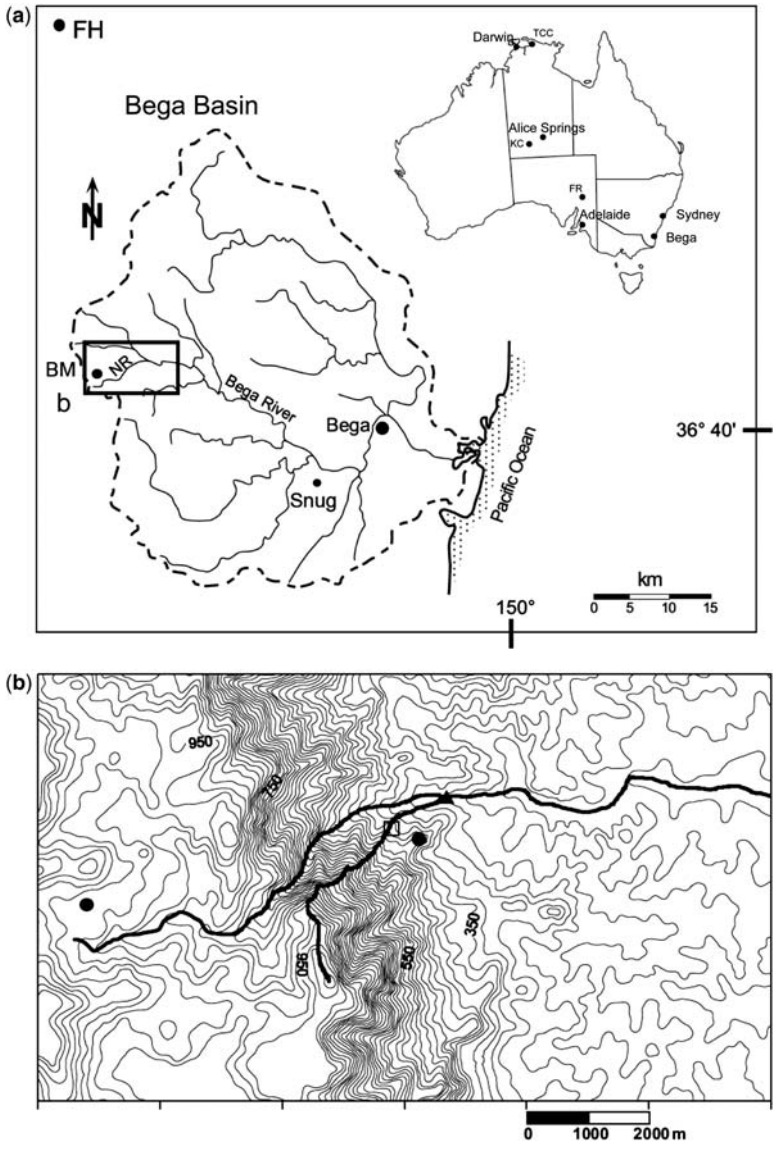

Fig. 1. (**a**) Bega Basin outline with field sites of previous work: FH, Frogs Hollow; BM, Brown Mountain; NR, Nunnock River; Snug, Snugburra. Inset shows outline map of Australia with cities nearest field sites of this paper. (**b**) Topography spanning the escarpment in the area shown by the rectangle in (a) with the transects used for sample collection shown. Contour interval is 20 m from the 1:100 000 digital data (Australian Surveying and Land Information Group) from Bega (sheet 8824) map. Modified from Heimsath *et al.* (2000) and showing locations used for that study (open square is approximate survey area; black dot on ridge crest is where the tor samples were collected; black triangle shows initial Nunnock River stream sediments). Other Australia sites: FR, Flinders Range; KC, Kings Canyon; TCC, Tin Camp Creek.

Brown Mountain (BM site). Cosmogenic nuclide determinations from all four sites together with an account of landscape evolution have been reviewed by Heimsath *et al.* (2006). Chemical weathering across the escarpment has been examined by Burke *et al.* (2009), whereas Braun *et al.* (2001), Heimsath *et al.* (2002, 2005) and Kaste *et al.* (2007) examined the physical mixing processes at NR.

In summary, the physiography of these sites is as follows. The NR site comprises convex spurs at Nunnock River, a bedrock channel that rises *c*. 1000 m above sea level in the tablelands and

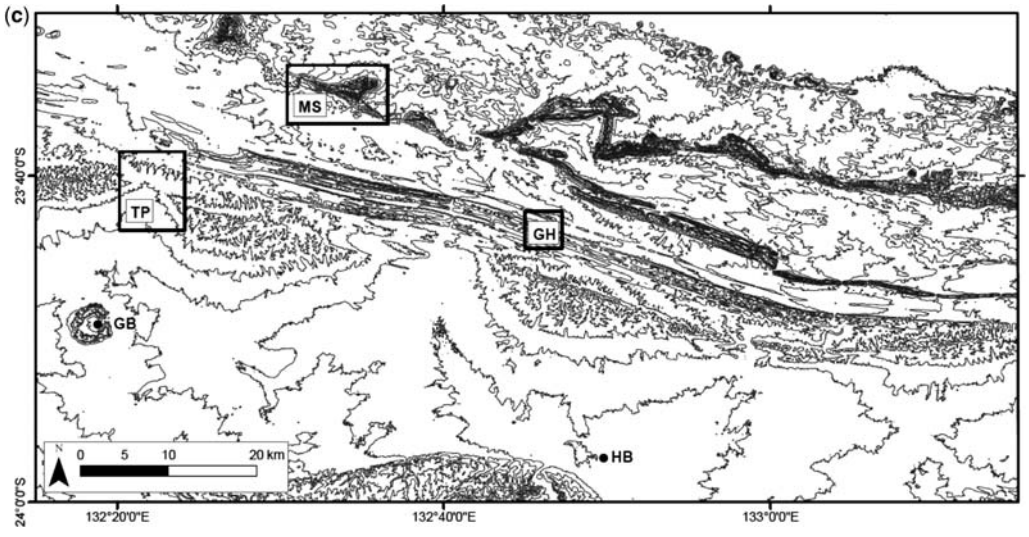

Fig. 1. (*Continued*) Other field site areas (TP, Tyler Pass; GH, Glen Helen; MS, Mount Sonder; shown in Figures 2, 6 and 7, respectively) are located by boxes in (**c**). The eastern border of the map is 70 km from Alice Springs. GB, Gosse Bluff; HB, Hermannsburg.

steeply descends the escarpment (Fig. 1a and b). The convex spurs are soil mantled and steepen downslope to intervening channels, which pass through very coarse, consolidated debris-flow deposits. Bedrock cliffs are prominent near the escarpment top, although they are less dramatic than those to the north in the New England Fold Belt described by Weissel & Seidl (1997, 1998), and are eroding by block failure on the escarpment face and by thin exfoliation and sheet erosion on top. Little sediment has accumulated beneath the cliffs and it appears that the upper region of the escarpment is weathering limited. From the escarpment base to the coast, the landscape is dominated by rolling hills of Late Silurian–Early Devonian granodiorite. Inland, tableland and ranges, dominated by Ordovician–Silurian metasediments and Devonian granites with extensive Tertiary basalt flows (Richardson 1976), lie *c*. 800–1500 m asl and typically have relatively gentle, soil-mantled slopes ($<25^{\circ}$), punctuated by frequent tors. Rainfall at the coastal lowlands site (Snug: 200 m asl, *c*. 900 mm a^{-1}) and at escarpment base (NR: *c*. 400 m; *c*. 1200 mm a^{-1}), is higher than on the highlands (FH: *c*. 900 m; *c*. 700 mm a^{-1}), and is distributed throughout the year (Richardson 1976; Australian Bureau of Meteorology: www.bom.gov.au/climate/averages). We refer to these areas as humid, temperate lowlands (NR and Snug) and cool highlands (FH and Brown Mt).

Central Australia: Tyler Pass. The western MacDonnell Ranges, west of Alice Springs in central Australia, are dominated by steep bedrock ridges in folded Palaeozoic and Precambrian quartzites, metasediments and gneisses. Unusual in this landscape, soil-mantled convex-up spurs occur on late Palaeozoic lithified conglomerate at Tyler Pass, about 150 km west of Alice Springs (Figs 1c and 2). Local relief of the spurs seen in Figure 2 is *c*. 20 m; hillslope lengths are *c*. 100 m, and slopes reach *c*. 25° as they approach dry bedrock channels that lie between them. The soil is strongly bioturbated and its thickness is almost uniform (*c*. 0.5 m). Tape and clinometer measurements showed that slope increases steadily downslope from ridge crests, indicating constant curvature. This geometry and constant-thickness soil suggest that ridge profiles have reached equilibrium.

Cosmogenic nuclide samples were collected from weathered rock below the soil base, and sand and pebbles were collected from local deposits in first- and second-order channels dissecting the hills, and from the dry bed of the main channel draining south from Tyler Pass.

Arnhem escarpment: Tin Camp Creek. The site is a soil-mantled basin in hard Precambrian sandstone, in the region of the Arnhem escarpment. A ridge, partly soil-mantled, bisects the basin: the soils are mostly red loamy earths and shallow gravelly loam with some micaceous silty yellow earths and minor solodic soils on the alluvial flats (Riley & Williams 1991). Bedrock exposures across the hills are significantly less weathered than saprolite beneath the soil mantle (Wells *et al.* 2008). Vegetation is open dry-sclerophyll forest interspersed

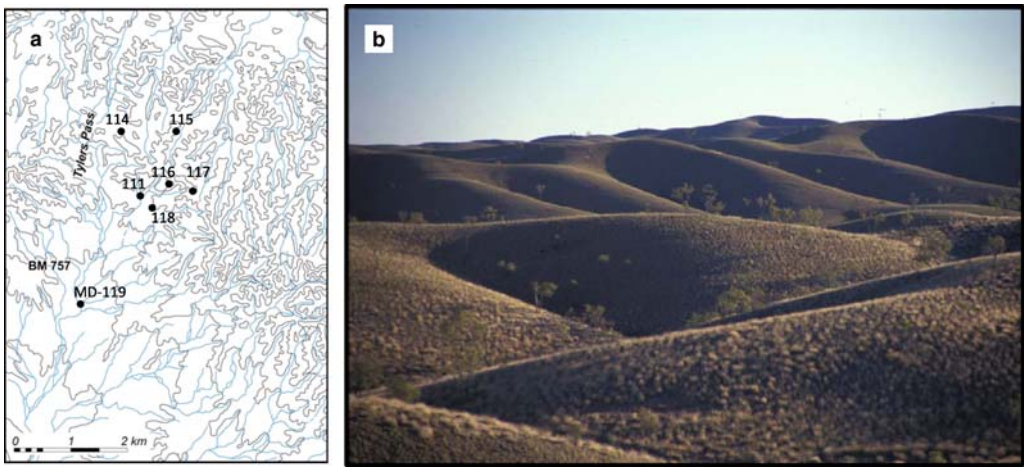

Fig. 2. (**a**) Tyler Pass field area. Contours and ephemeral streams extracted from Australian Surveying and Land Information Group (AUSLIG) draft map, 5350: Gosse Bluff. Elevation at pass is 815 m; 20 m contour intervals. MD sample numbers label approximate sample locations. MD-119 is at 23°41.795′S, 132°21.246′E. (**b**) Photograph of the soil-mantled hills of Tyler Pass.

with seasonal tall grassland; tree-throw and burrowing animals contribute to soil transport, and feral water-buffalo and pigs have caused local erosion (Riley & Williams 1991; Hancock *et al.* 2000; Townsend & Douglas 2000; Saynor *et al.* 2004, 2009; Staben & Evans 2008). Rainfall is *c.* 1400 mm a^{-1}, falling almost entirely between October and April, typically in short, high-intensity storms. The climate is classed as monsoon–tropical.

Tin Camp Creek is undisturbed by colonial land use and, as it closely resembles the terrane at Energy Resources Australia Ranger uranium Mine (ERARM), where geomorphological processes and rates are of high interest, is a site of intensive study. Fieldwork was carried out by A.H. in collaboration with G. Hancock of the Office of the Supervising Scientist, Jabiru, and D. Fink of the Australian Nuclear Science and Technology Organisation (Heimsath *et al.* 2009). Our sampling traversed the central ridge, with samples of both exposed and unweathered bedrock as well as weathered rock from below a range of soil depths, together with catchment sediment samples, to assess the spatial variability of erosion rates across a landscape that is used as a reference site by the uranium mining industry (Hancock & Evans 2006; Hancock *et al.* 2008*a*, *b*; Fig. 3).

Bedrock-dominated landscapes

Flinders Ranges. The Flinders Ranges in South Australia, flanked by the great salt playas of lakes Frome, Eyre and Torrens, are dominated by Late Proterozoic rocks, moderately to steeply dipping, from very hard quartzites through sandstones and limestones to comparatively friable quartzose mudstones. The Ranges rise to over 600 m and are structurally controlled, varying from high quartzite ridges to rounded hills and cuestas in cyclic sandstone–shale–limestone sequences. Seismic activity and evidence of late Cenozoic thrusting suggest continuing tectonic uplift (Quigley *et al.* 2007*a*, *b*), although the rate has yet to be determined and probably is slow. Regional climate is semi-arid, with mean annual precipitation ranging from 250 mm a^{-1} at Port Augusta to over 400 mm a^{-1} in the Ranges.

Our study area centres on Brachina and Parachilna Creeks, bedrock channels that flow westward from the diapiric core of the Ranges through cuestas and rounded ridges of cyclic sandstone and mudstone, and then pass through deep, steep-sided gorges cut in hard sandstone and quartzite. Slope erosion is dominated by shedding of joint-controlled blocks. There is no continuous detrital cover, and the slopes are weathering-limited. Rock surfaces are reddened by iron oxides, suggesting relatively slow slope retreat, and falling blocks tend to disintegrate during their downslope passage. West of the gorge, the wide, boulder-strewn channels form fans and dwindle as they head towards playa-lake Torrens.

We collected samples around the gorges of Brachina and Parachilna Creeks (Fig. 4), from steep to precipitous slopes in jointed quartzite (Brachina gorge) and sandstone (both gorges), to determine erosion rates of weathering-limited slopes and also to assess the variation of cosmogenic nuclides in

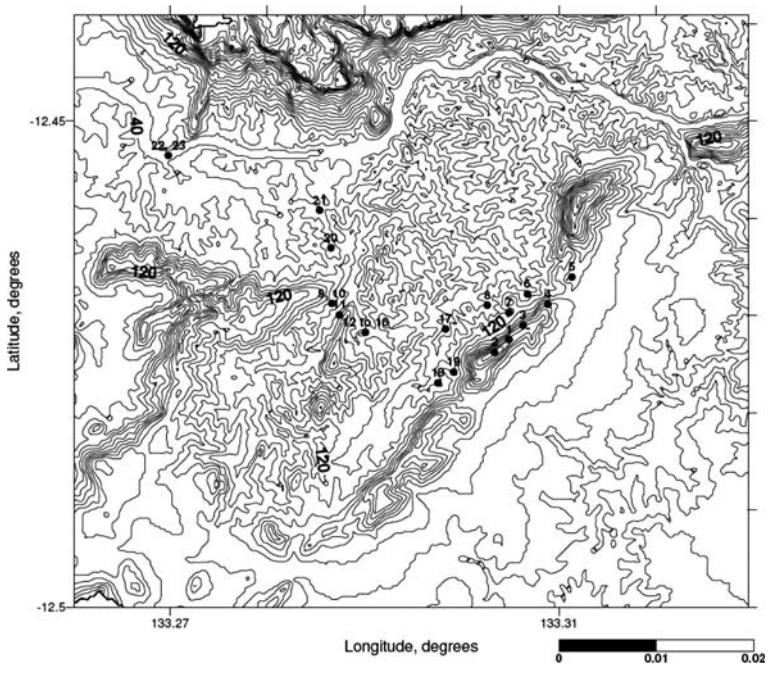

Fig. 3. Contour map and sample locations for Tin Camp Creek (TCC) field area of Heimsath *et al.* (2009). Topography extracted from regional digital elevation model (e.g. Hancock & Evans 2006); 10 m contour intervals. Sample locations shown with black dots and (TC) number of Heimsath *et al.* (2009). Samples 22 and 23 mark the main drainage of TCC.

point samples from joint-controlled rocky slopes. We also sampled quartzite gravel and bedrock knickpoints in low-order channels.

Central Australia: Kings Canyon. Carved in gently dipping Late Palaeozoic sandstone (Bagas 1988), the bedrock-dominated inner drainage basins in Kings Canyon National Park include regularly spaced, convex-up bedrock ridges with relatively steep slopes (Fig. 5) that are remarkably similar in form to steep, soil-mantled landscapes of coastal Oregon (Heimsath *et al.* 2001*b*; Roering *et al.* 2001), despite the fact that Kings Canyon lies in arid, tropical central Australia and receives only *c*. 260 mm a^{-1} of rainfall.

The regularly spaced convex ridges pose a geomorphological puzzle. Evolution of convex ridges under a soil mantle is expected with diffusive soil creep and depth-dependent soil production (Heimsath *et al.* 1997, 2000), but it is unclear how these forms could develop in weathering-limited bedrock landscapes, eroding by processes acting on steep rectilinear and concave slopes of the Flinders Ranges. Conjecturing that the convex ridges may have formed under a soil mantle during wetter climate in the past, we hypothesize that present-day erosion rates are inconsistent with evolution of the observed topography, and collected samples downslope as shown in Figure 5.

Central Australia: Mt Sonder and western MacDonnell Ranges. The MacDonnell Ranges are dominated by steep, structurally controlled bedrock ranges: quartzites form high, precipitous rectilinear slopes, whereas sandstone and other rocks tend to be dissected in parallel, convex-up rounded spurs similar to those of Kings Canyon. The climate is semi-arid, similar to that of Kings Canyon, with *c*. 2–300 mm a^{-1} highly variable rainfall. Spinifex (*Triodea*) and other grasses together with intermittent acacia and eucalyptus shrubs and trees mantle the stony landscape. In addition to Tyler Pass, described above, we selected two other field sites to assess the effect of lithology on erosion rates: one at Glen Helen in Hermannsburg Sandstone (Figs 1c and 6) and the other on Mt Sonder in Heavitree Quartzite (Figs 1c and 7). Both are bedrock-dominated; erosion processes are similar to those in the Flinders Ranges, outlined above, and both are characterized by rounded bedrock ridges with no soil mantle. Despite the clear differences in rock hardness, the two sites are morphologically

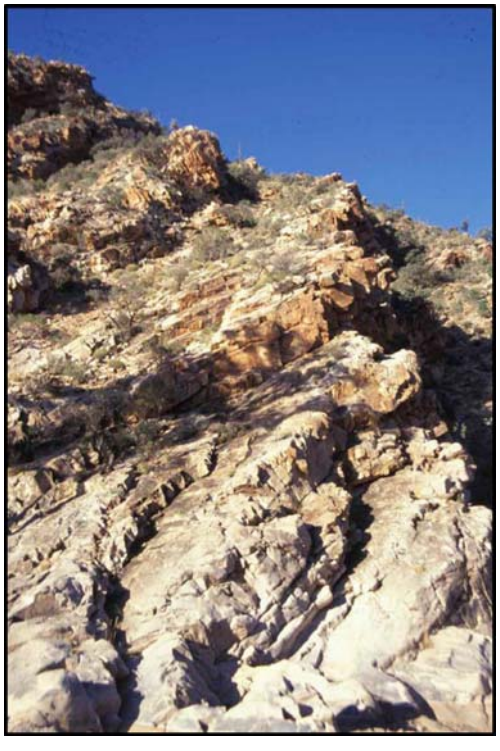

Fig. 4. Photograph of the Flinders Range blocky cliff exposure used to calibrate a bedrock erosion model. Samples collected from above and below the bedrock steps shown in the photograph were compared with average erosion rates from low-order stream sands draining catchments adjacent to this ridge.

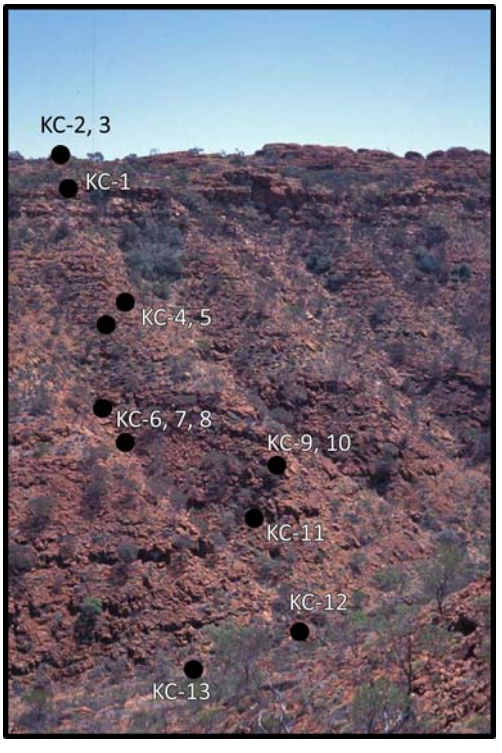

Fig. 5. Photograph of the bedrock ridge–valley topography of Kings Canyon with approximate sample locations shown with black filled circles. Samples were collected from the 'beehive'-shaped features of the Mereenie Sandstone at the top of the ridge, down the axis of the central ridge of the photograph, with some samples from the active channels.

similar, with maximum spur-crest slopes of *c*. 35°. Local relief is *c*. 200 m at the Glen Helen site (Fig. 6) and ranges from 250 m to >500 m at Mt Sonder (Fig. 7).

Results

Soil-mantled landscapes

Rates of soil production. Soil production and transport are considered to be in steady state at the NR and Snug sites in humid southeastern Australia. In their intensive study at the NR site, Heimsath *et al.* (2000) showed that soil thickness is negative-exponentially dependent on slope curvature, and we have confirmed a similar relationship at Snug. Moreover, cosmogenic nuclide concentrations in granite tors at NR reveal uniform-rate lowering of the surrounding soil (Heimsath *et al.* 2000). Cosmogenic measurements from beneath soil base robustly define an exponential decline of the soil production with increasing soil thickness; as reported previously

$$\varepsilon(H) = 53 \pm 2e^{-(0.022 \pm 0.001)H} \quad (4)$$

where $\varepsilon(H)$ is soil production rate (m Ma^{-1}) and H is soil thickness (cm). Results from Brown Mountain and FH also accord with this relationship (Fig. 8a), although it must be noted that the FH site at 900 m asl probably is not in steady state, having almost certainly been affected by periglacial solifluction (Heimsath *et al.* 2001*a*).

Turning to tropical Australia, measurements of soil production and soil thickness at Tin Can Creek (TCC) in the monsoonal far north (Heimsath *et al.* 2009) overlap completely with those from our southeastern sites, as Figure 8 shows, except that the TCC rates are lower where soil thickness approaches zero and suggest a 'humped' production function; Wilkinson *et al.* (2005) proposed a similar

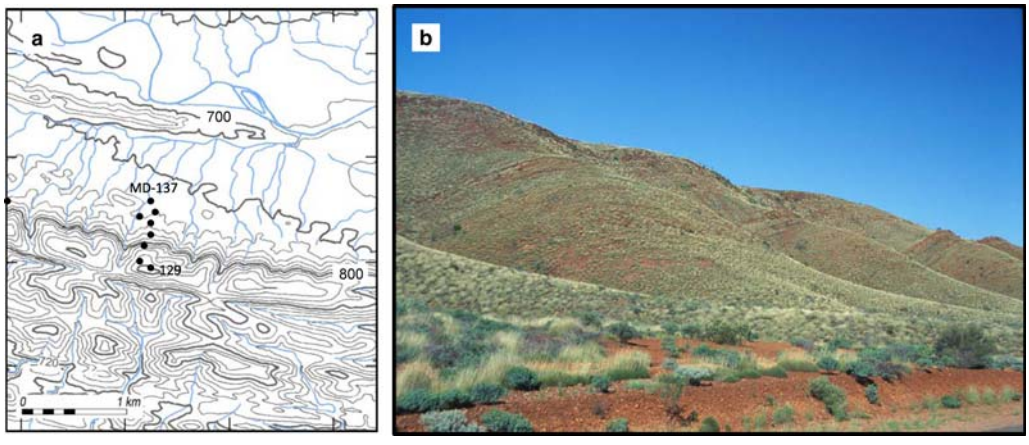

Fig. 6. (**a**) Glen Helen field area. Contours and ephemeral streams extracted from Defense Imagery and Geospatial, 1:100 000 map Series R621, Sheet 5550: MacDonnell Ranges; 20 m contours. MD sample numbers label approximate sample locations. MD-130 sampled near 129 and MD-137 is at 23°42.501′S, 132°46.443′E. (**b**) Photograph of the ridge from the Alice Springs–Tyler Pass Road, looking SW. Despite the soil-mantled appearance, these hills are almost entirely bedrock, albeit a fractured and weathered bedrock able to support ample vegetation.

relationship in the Blue Mountains, SE Australia. That landscapes with such different climates show such similar soil production functions seems surprising but suggests that similar processes, presumably dominantly biotic, are instrumental in producing and transporting soil. Measurements of rates of soil-particle migration would be informative, similar to those reported from NR by Heimsath *et al.* (2002). In contrast, soil production on spurs at Tyler Pass in semi-arid central Australia is significantly lower: rates of 6.6–6.7 m Ma^{-1} were obtained at five pits, under soil thicknesses of 28–35 cm (Table 1; Fig. 8). For comparable thicknesses at both the monsoonal and southern sites, the rate is 30–35 m Ma^{-1}. Moreover, the mean erosion rate at Tyler Pass, determined from sand and pebble samples from nearby channels, is also 6–7 m Ma^{-1} (Table 2). We presume the difference between semi-arid Tyler Pass and both the monsoonal and the southeastern sites reflects the effect of soil moisture on both chemical weathering and biotic activity.

Exposed rock at soil-mantled sites. Local exposures of bedrock occur at our granitic soil-mantled sites in SE Australia, and at the monsoonal tropical sandstone site (TCC), either as upstanding tors (emergent corestones) or as flat exposures that pass beneath soil at their edges: the data are represented in Figure 8 as points at zero soil thickness. Erosion

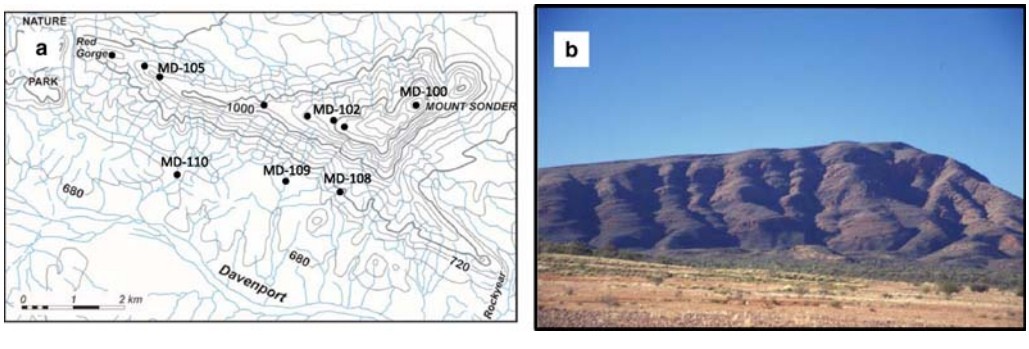

Fig. 7. (**a**) Sonder field area. Contours and ephemeral streams from Australian Surveying and Land Information Group (AUSLIG) draft map, 5450, Hermannsburg; 40 m contours. MD sample numbers label selected approximate sample locations. MD-100 is at 23°34.860′S, 132°34.238′E. (**b**) Photograph of Mt Sonder from the Alice Springs–Tyler Pass Road, looking NE. The highest point (*c.* 1320 m elevation) is not visible.

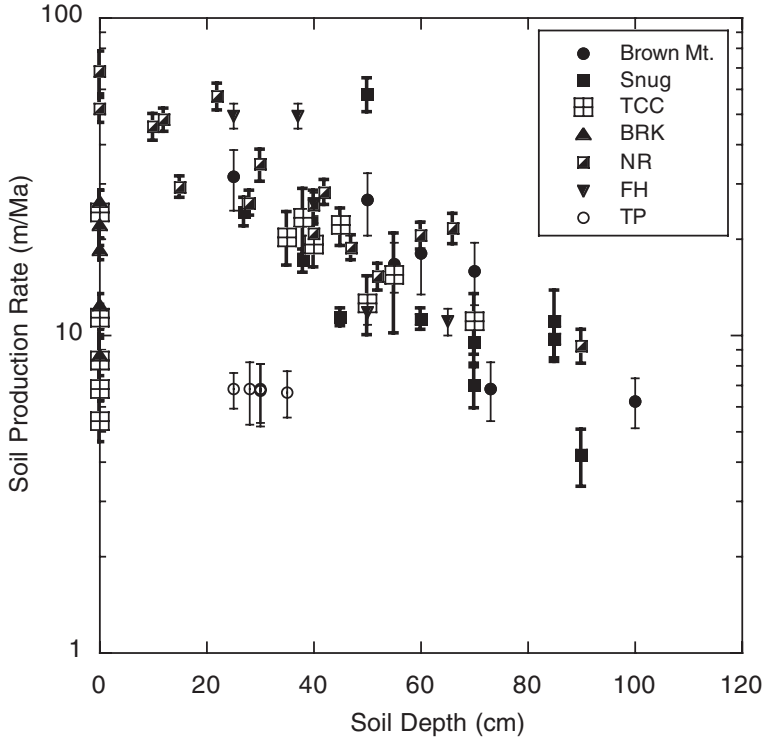

Fig. 8. Soil production rates plotted against overlying soil thickness for all four field sites across the southeastern escarpment (NR, Nunnock River; FH, Frogs Hollow), as well as the seven soil production rate samples collected from beneath soil at Tin Camp Creek (TCC). Additionally, soil production rates from the five Tyler Pass samples, with little variation in soil depth, are plotted with open circles.

rates determined from these exposures show a considerable range (5–60 m Ma^{-1}), some being higher and others much lower than results from nearby soil-covered sites. Erosion is by grain-by-grain disintegration at all these sites and the wide spread of results is not attributable to episodic shedding of coarse blocks, but reflects the position of each sample relative to the nearby soil. As Heimsath *et al.* (2000, 2001*a*, *b*) described, rates similar to values from beneath thin soil generally came from flat exposures at soil level, whereas the low erosion rates were obtained from the sides and tops of tors.

Topographic variation of erosion rates. Our erosion-rate measurements from the escarpment that rises from NR to Brown Mountain are strongly altitude dependent. The dataset includes eight samples from small, zero- and first-order streams draining the escarpment, 10 samples from beneath shallow soil on a downhill line on a prominent spur, three samples from granite tor-tops from the escarpment crest, and three samples from the tops of granite cliffs along the steep escarpment face. Rates at a given elevation are consistent between soil-mantled samples, sediments and bedrock samples. These 24 samples together with the average erosion rate from NR show a strong trend of increasing erosion rate with decreasing altitude (Fig. 9a), from *c.* 3 m Ma^{-1} at the escarpment top to *c.* 35 m Ma^{-1} near the base. There is no relationship between erosion rate and either local slope or basin-averaged slope, which may be due to the lack of relationship between soil thickness and slope as discussed further by Burke *et al.* (2009). Extrapolated to million year time scales, these results imply that the escarpment scarp becomes steeper with time, unless corrected by some process not measured by these data. Not only is it unlikely that the escarpment will become indefinitely steeper but long-term constancy of form is supported by apatite fission-track and (U–Th)/He data (Persano *et al.* 2002, 2005). It seems likely that the very coarse diamictites observed in the ravines near the escarpment base (Heimsath *et al.* 2000, 2006) represent large mass-movements that episodically reverse the trend suggested by Figure 9a.

The TCC data from the tropical monsoonal north show a rather similar pattern. The relief is less than

Table 2. *Erosion rates from cosmogenic nuclide concentrations*

Sample	Weight (g)	Carrier (μg)	^{10}Be (10^6 atoms g^{-1})	Prod. rate	Elev. (m)	E (m Ma^{-1})	Min. exp. (ka)
Kings Canyon							
KC-1	27.49	447	17.052 ± 0.886	6.54	789	0.24 ± 0.03	2607
KC-2	30.34	383	22.379 ± 1.045	6.56	793	0.18 ± 0.02	3411
KC-3	29.18	383	14.124 ± 0.612	6.55	791	0.24 ± 0.03	2156
KC-4	30.07	428	9.719 ± 0.412	6.36	750	0.39 ± 0.04	1528
KC-5	28.82	442	3.792 ± 0.188	6.29	735	0.99 ± 0.12	603
KC-6	30.57	465	1.509 ± 0.178	6.20	715	2.43 ± 0.51	243
KC-7 S	28.45	424	2.109 ± 0.163	6.16	705	1.73 ± 0.27	342
KC-8 P	30.19	434	13.907 ± 0.555	6.13	700	0.26 ± 0.03	2269
KC-9	29.53	398	1.237 ± 0.115	6.08	687	2.97 ± 0.54	204
KC-10	29.62	416	1.880 ± 0.136	6.07	685	1.95 ± 0.30	310
KC-11	31.09	411	1.501 ± 0.148	6.02	675	2.32 ± 0.44	249
KC-12 S	29.92	412	1.026 ± 0.067	5.86	638	3.38 ± 0.51	175
KC-13 P	29.75	469	1.797 ± 0.289	5.85	635	1.93 ± 0.53	307
Mt. Sonder							
MD-100	30.08	445	2.189 ± 0.162	9.42	1320	2.00 ± 0.23	232
MD-101	29.76	469	3.675 ± 0.266	8.90	1240	1.51 ± 0.13	413
MD-102	30.62	458	2.505 ± 0.419	8.53	1180	1.79 ± 0.35	294
MD-103	29.32	456	3.235 ± 0.384	8.21	1125	1.58 ± 0.21	394
MD-104	29.62	440	1.428 ± 0.168	7.67	1030	2.77 ± 0.48	186
MD-105	30.60	478	7.026 ± 0.399	7.21	945	0.76 ± 0.06	974
MD-106	30.64	457	2.992 ± 0.193	7.19	940	1.60 ± 0.15	416
MD-107	29.95	437	1.555 ± 0.115	7.03	910	2.51 ± 0.32	221
MD-108 S	29.88	433	5.605 ± 0.254	6.75	770	0.80 ± 0.07	830
MD-109 S	30.83	425	1.299 ± 0.111	6.75	700	2.84 ± 0.42	192
MD-110 S	28.54	300	4.001 ± 0.286	6.60	675	1.47 ± 0.12	606
Tyler Pass							
MD-111 S	30.15	409	0.636 ± 0.102	6.47	792	6.14 ± 1.30	98
MD-112 P	31.37	387	0.671 ± 0.120	6.48	794	5.83 ± 1.34	104
MD-114 (35 cm)	29.66	417	0.618 ± 0.071	6.56	810	6.61 ± 1.08	94
MD-115 (30 cm)	29.44	417	0.283 ± 0.049	6.51	801	6.67 ± 1.49	44
MD-116 (25 cm)	20.73	447	0.211 ± 0.016	6.53	804	6.76 ± 0.84	32
MD-117 (28 cm)	30.39	352	0.360 ± 0.061	6.51	799	6.75 ± 1.48	55
MD-118 (30 cm)	30.80	393	0.488 ± 0.079	6.61	822	6.75 ± 1.41	74
MD-119 S	28.52	359	0.498 ± 0.041	6.33	760	7.12 ± 1.35	64
MD-119 P	31.39	437	0.624 ± 0.148	6.33	761	5.68 ± 1.68	99
Glen Helen							
MD-129	29.35	397	1.362 ± 0.183	7.00	900	3.20 ± 0.55	217
MD-130	29.89	329	2.245 ± 0.307	7.00	900	1.94 ± 0.34	357
MD-131	29.70	390	0.287 ± 0.075	6.95	890	14.34 ± 4.16	46
MD-132	30.65	394	0.820 ± 0.135	6.70	838	4.99 ± 1.04	132
MD-133	29.48	379	0.343 ± 0.047	6.35	765	11.00 ± 2.12	56
MD-135	30.17	366	0.350 ± 0.062	6.15	720	10.51 ± 2.52	58
MD-136	29.40	367	0.867 ± 0.166	6.12	715	4.29 ± 1.10	143
MD-137	29.78	338	0.543 ± 0.075	6.06	700	6.68 ± 1.35	90
Flinders Range							
Blocky quartzite slopes							
Br8U2	33.74	454	1.140 ± 0.130	6.22	400	2.2 ± 0.28	183
Br9i	31.83	365	0.600 ± 0.050	6.22	400	4.36 ± 0.41	96
F108P	32.17	456	0.570 ± 0.040	6.40	380	5.92 ± 0.44	89
FR9	31.22	460	0.550 ± 0.040	7.20	460	6.31 ± 0.46	76
FR11	16.76	309	0.590 ± 0.070	7.04	445	6.37 ± 0.8	84
Br8U1	30.37	374	0.320 ± 0.040	6.22	400	8.32 ± 0.97	51
FR10	31.29	383	0.290 ± 0.020	6.94	350	10.82 ± 0.87	42
FR12	31.45	380	0.350 ± 0.030	7.04	470	10.81 ± 0.96	50
FR7	23.09	306	0.290 ± 0.060	6.89	400	11.37 ± 2.7	42

(*Continued*)

Table 2. *Continued*

Sample	Weight (g)	Carrier (μg)	^{10}Be (10^6 atoms g^{-1})	Prod. rate	Elev. (m)	E (m Ma^{-1})	Min. exp. (ka)
Quartzite sediments							
F109s	21.25	316	0.900 ± 0.050	6.40	350	3.66 ± 0.22	141
P499	31.10	356	0.790 ± 0.050	7.04	380	5.12 ± 0.31	112
Br399	30.11	457	0.660 ± 0.040	7.14	375	5.15 ± 0.33	92
F109P	23.32	300	0.540 ± 0.040	6.40	350	6.27 ± 0.49	84
F110s	30.51	366	0.530 ± 0.050	7.96	325	7.6 ± 0.75	67
Rocky sandstone slopes							
P399	30.62	312	0.520 ± 0.024	7.14	390	7.31 ± 0.35	73
FR4	29.98	350	0.410 ± 0.060	6.89	400	9.1 ± 1.39	60
P299	31.58	353	0.270 ± 0.040	7.14	375	14.07 ± 2.37	38
P199	31.28	354	0.220 ± 0.020	6.89	350	16.35 ± 1.46	32
P199	31.10	356	0.210 ± 0.020	6.89	350	17.06 ± 1.68	30
FR5	30.55	344	0.150 ± 0.020	6.89	400	21.91 ± 3.54	22

All errors propagated to erosion rate, E; Min. exp. is the minimum exposure age to cosmic-ray flux. Production factor scales nuclide prodution for slope, soil cover, elevation and latitude. Calculated using Cronus online calculator (http://hess.ess.washington.edu/math/). S and P, sand and pebbles, respectively, referring to catchment-averaged detrital sediment samples. [For Tin Camp Creek data see Heimsath *et al.* (2009)]. For Bega Valley data see Heimsath *et al.* (2000, 2001*a*, 2006).

that of the southeastern escarpment (200 m v. 800 m) but the physiography is similar, with soil-mantled convex spurs below rocky cliffs, topped by ridge-and-plateau terrain. Figure 9b plots erosion rates v. altitude, determined from soil-mantled spurs, exposed bedrock, and sediments from small channels. Excepting two sediment samples from the lowlands, the results suggest decreasing erosion rate with increasing elevation, from *c*. 20 m Ma^{-1} at 80 m asl to *c*. 5 m Ma^{-1} at 230 m asl. As with the southeastern escarpment, the pattern implies that slopes around TCC become progressively steeper through time, unless the trend is reversed by processes not apparent today.

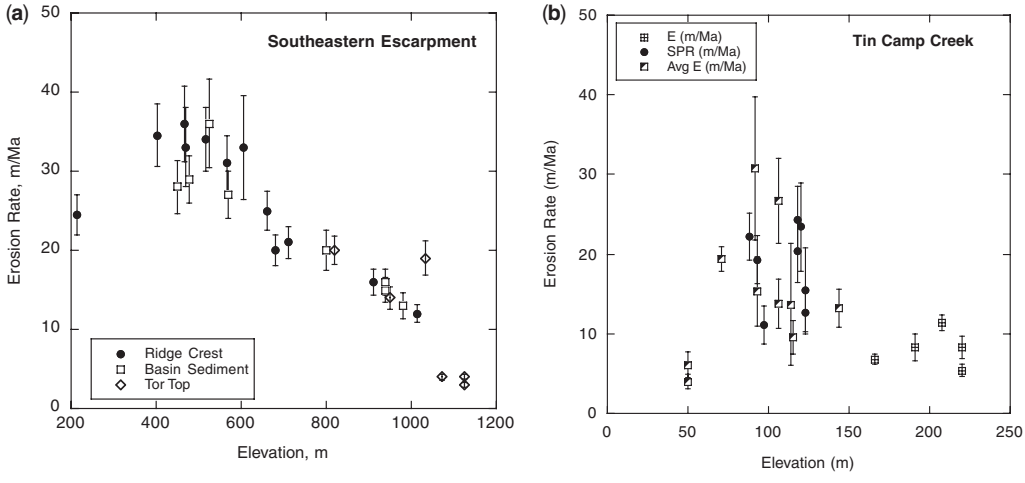

Fig. 9. (**a**) Erosion rates from ridge crest (filled black circles), small catchment (open squares) and tor top (open diamonds) samples plotted as a function of elevation across the southeastern escarpment face. For most of the samples, the ridge-crest and small catchment samples were adjacent for similar elevations. Average values for the soil production rates at the scarp base (NR) and the coastal lowland (Snug) sites are included. (**b**) Soil production (filled black circles), average erosion (half-filled squares) and point-specific bedrock erosion (open squares with crosses) plotted against elevation for the Tin Camp Creek field site. Lowest elevation samples are from the Tin Camp Creek, draining the entire field area, as well as the extensive stony highlands. Adapted from Heimsath *et al.* (2009).

Bedrock-dominated landscapes

Erosion in the steep, weathering-limited bedrock slopes and ridges that we examined in the Flinders and MacDonnell Ranges is dominated by joint-controlled break-up on stratified and schistose rock surfaces, and by exfoliation and granular disintegration on massive, coarsely crystalline plutonic rocks. Clasts and grains drift downslope, disintegrating further as they go and lodging temporarily in joint-angle pockets but, on the slopes we sampled, not in sufficient quantities to form talus slopes or colluvial mantles. Vegetation patches of herbs, grasses and shrubs pattern the slopes, rooted in loose gravelly sand. Drainage is focused by steep bedrock channels, with discontinuous alluvial deposits of mixed sand, gravel and angular boulders, interrupted by knickpoints. Although physiographically similar, the Flinders and MacDonnell Ranges yielded somewhat different results, and are summarized separately.

Erosion rates on different rock-types. (i) Flinders Ranges. We sampled *in situ* rock surfaces on steep, coarsely jointed quartzite slopes (joint spacing 60 cm) (nine samples), sediments derived from these slopes (five samples), and rocky sandstone slopes (five samples). Results are listed in Table 2. Erosion rates calculated from ^{10}Be measurements for quartzite samples varied: surfaces that appeared to have been exposed by slip-off of overlying blocks gave the highest apparent rates (FR7, FR10, and FR12) whereas surfaces judged to have been long exposed, from their state of red-weathering, gave the lowest apparent rates (Br8U2, BR9i). The mean of the measurements from rock surfaces is 7.4 m Ma^{-1}; the range (2.2–11.4 m Ma^{-1}) is similar to that predicted using equations (2) and (3) with block size $L = 60$ cm (1.8–9.5 m Ma^{-1}). Standard deviation and standard errors are ± 3.2 and ± 1.1, respectively. The mean rate from quartzite sand and gravel channel sediments is 5.6 m Ma^{-1} (standard error ± 0.7 m), statistically similar to the average for the *in situ* samples, suggesting that (1) the average erosion rate obtained from the *in situ* samples is a reasonable estimate, and (2) exposure to cosmic rays as weathered clasts move from the rocky slopes into stream sediments is minor, relative to *in situ* exposure before break-out from the slope; that is, the travel time is relatively short for these landscapes.

Erosion rates from *in situ* sandstone samples are significantly higher than from the quartzite, ranging from 7.3 to 21.9 m Ma^{-1} with a mean of 14 $\pm$ 2 m Ma^{-1}. Extrapolation back over tens of millions of years suggests that sandstone ridge-crests should be substantially lower than quartzite crests. Although this is locally the case in the neighbourhood of Brachina and Parachilna gorges, it is not so throughout the Flinders Ranges as a whole, suggesting continuing, slow differential uplift. Quigley *et al.* (2007*a*, *b*) reached a similar conclusion at faulted terrain in the central Flinders Ranges.

(ii) MacDonnell Ranges and Kings Canyon. Long, convex-up spurs in jointed bedrock were sampled in the western MacDonnell Ranges, in quartzite at Mt Sonder and sandstone at Glen Helen, and in sandstone at Kings Canyon. Surface erosion rates measured at Mount Sonder are consistently low, ranging from 0.7 to 2.8 m Ma^{-1} (eight samples: Table 2) with a mean of 1.8 $\pm$ 0.2 m Ma^{-1}. Three sediment samples from small bedrock channels give essentially the same result: 1.7 $\pm$ 0.6 m Ma^{-1}. Surface erosion rates from the Glen Helen sandstone site are both higher and more scattered, ranging from 1.9 to 14.3 m Ma^{-1} (six samples) with a mean of 6.6 $\pm$ 2.0 m Ma^{-1}. In contrast, erosion rate measurements from Kings Canyon sandstone site are low, ranging from 0.18 to 2.97 m Ma^{-1} (nine samples), with a mean of 1.3 $\pm$ 0.4 m Ma^{-1}. Four sediment samples from small bedrock channels give a similar result: 1.8 $\pm$ 0.6 m Ma^{-1}.

Topographic variation of erosion rate

In contrast with the high, soil-mantled escarpment in humid SE Australia, where erosion rate declines markedly with increasing altitude, we found no regular variation of erosion rate with altitude at our sites in semi-arid central Australia. Although the variability inherent in point measurements from coarsely jointed surfaces will tend to mask trends, we consider that overall there are sufficient measurements for any trends to be apparent, if present. Allowing for inherent scatter, erosion rates at Mt Sonder, which has both the greatest relief and the most measurements, effectively are the same at all altitudes, from the base at *c*. 700 m asl to the top at 1350 m asl (Fig. 10a). Results from Glen Helen are too scattered for any trend to be revealed (Fig. 10b), whereas at Kings Canyon, erosion rates appear to drop in a step-like manner, from *c*. 2 m Ma^{-1} below *c*. 720 m asl to $<$0.5 mMa^{-1} above 720 m (Fig. 10c).

Discussion

Ranking the sites in ascending order in terms of erosion rates (means and standard errors in m Ma^{-1}), we have: Kings Canyon sandstone (1.5 $\pm$ 0.3); Mt Sonder quartzite (1.8 $\pm$ 0.2); Tyler Pass conglomerate (6.5 $\pm$ 0.2); Flinders Ranges quartzite (6.7 $\pm$ 0.7); Glen Helen sandstone (7.1 $\pm$ 1.5); Flinders Ranges sandstone (14 $\pm$ 2);

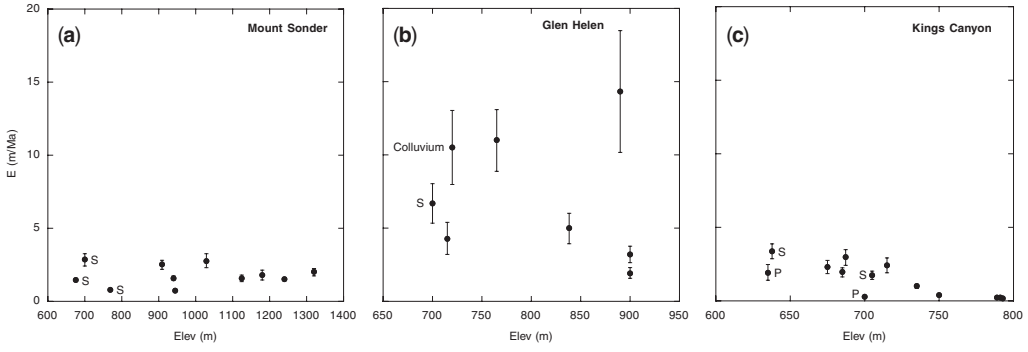

Fig. 10. Bedrock erosion rates from point-specific samples, as well as average erosion rates from sediment samples, plotted as functions of sample elevation. (**a**) Rates from Mount Sonder are roughly equal, with the lowest erosion rates from sampled tor surfaces on the ridge crest. The three lowest elevation samples are catchment-averaged rates from sands collected in different drainages (Fig. 7a). (**b**) Rates from the Glen Helen ridge transect show greater scatter. S, sand draining the ridges in first-order drainage. (**c**) Rates from Kings Canyon range from almost zero at the top to average rates from the sediments roughly equivalent to the Mount Sonder field area, roughly 100 km north. Sand (S) samples show higher erosion rates than pebble (P) samples collected at same location.

monsoonal north, TCC sandstone (14 ± 4); SE highlands, Brown Mt and FH granodiorite (14 ± 3); SE lowlands, NR and Snug granodiorite (35 ± 6). A number of factors affecting erosion rate emerge from this ranking: climate, presence or absence of soil, and rock type. Climatic history may also be a factor.

A climatic influence seems obvious (see Fig. 11). The average rates are lowest at Kings Canyon and Mt Sonder in semi-arid central Australia and are comparable with those reported for other semi-arid Australian sites, including inselbergs on the Eyre Peninsula in South Australia (Bierman & Caffee 2002) and the Davenport Range in the Northern Territory (Belton *et al.* 2004). In contrast, the rates are about 20 times higher at the NR and Snug sites in the temperate SE. Moreover, the low and high erosion rates parallel the absence or presence of a soil mantle: at the low end (the weathering-limited case), the supply of weathered detritus is less than the capacity of sliding, rolling and wash processes to move it downslope; at the high end (the transport-limited case), the supply exceeds the capacity of these simple processes and, as a result, a detrital blanket ('soil') builds up until downslope motion of the entire mantle equilibrates with supply, which in turn is mediated by the dependence of soil production on soil thickness [as shown by equation (4)]. Thus, climate, or, more exactly, moisture and temperature, governs both weathering rate and the balance of erosional processes, at least at the semi-arid and humid temperate ends of the spectrum.

Between these extremes, the effects of climate on weathering rates and presence or absence of soil are more blurred. Although rock hardness and jointing density appear to have an effect, as shown by the difference between neighbouring rocky quartzite and sandstone slopes in the Flinders Ranges (6.7 ± 0.7 v. 14 ± 2 m Ma^{-1}), other factors as well as climate influence both erosion rate and presence or absence of soil. For example, Tyler Pass and Glen Helen sites are convex-up spurs with similar mean erosion rates (6.5 and 7.1 m Ma^{-1}), but TP is soil-mantled whereas GH is not: the difference cannot be attributed to climate, which is the same

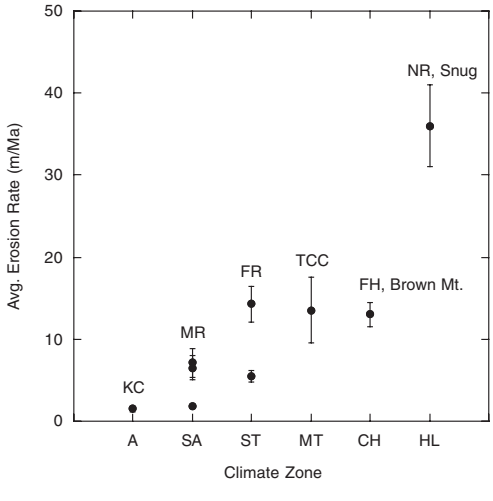

Fig. 11. Average erosion rate plotted against the climate zone characterizing each field site and labelled with the field site represented. A, arid (KC, Kings Canyon); SA, semi-arid (MR, MacDonnell Range); ST, semi-arid–temperate (FR, Flinders Range); MT, monsoonal tropic (TCC, Tin Camp Creek); CH, cool highland (FH, Frogs Hollow); HL, humid lowland (NR, Nunnock River).

at both sites. Furthermore, three other sites have similar mean erosion rates (*c*. 14 m Ma^{-1}) but different climates and cover; one is the bare, rocky Flinders Ranges sandstone, whereas two others are soil-mantled: TCC sandstone in the monsoonal north and the SE highland sites at Brown Mt and FH. We conclude that the threshold between weathering- and transport-limited slopes must depend not only on the rate of production of weathered detritus but also on local factors such as slope angle, runoff intensity and vegetation recruitment. However, without further studies at the field sites, we cannot resolve these effects.

Climatic history may be a confounding factor, if climate shifts led to changes of detrital or soil cover, which may be the case at some of our climatically mid-range sites on Late Quaternary time scales. In the SE highlands, for example, it is likely that soil locally was stripped during Late Quaternary glacial periods by periglacial processes (Heimsath *et al.* 2001*a*) that were active in the SE highlands, in which case erosion rates calculated using present-day soil thicknesses would be minimum estimates. Conversely, if sites that today are bare rock were blanketed by aeolian dust or sand in Late Quaternary times, as Williams *et al.* (2001) suggested for parts of the Flinders Ranges, then the calculated erosion rates will be maximum estimates.

We turn to the question of whether the observed erosional processes, acting at the measured rates, have generated the landforms observed today. This is strongly supported by our detailed studies at the soil-mantled lowland sites in humid southeastern Australia, where erosion rates are relatively rapid (Heimsath *et al.* 2000, 2002) and arguably is the case at the monsoonal tropical TCC site, but seems unlikely at the central Australian sites that have very low erosion rates. With a rate of 1–2 m Ma^{-1}, surface lowering since Late Miocene times would amount to only 10–20 m, which is small compared with the scale of the major spurs at Mt Sonder, for example. Surface conditions have changed over the last several million years at all our sites in the semi-arid region (as reviewed by Fujioka & Chappell 2010). In the Miocene, continuous forest cover throughout Australia gave way in the central regions to sclerophyll woodland and savannah; alkaline lakes developed accompanied by dissection and alluvial fan activity, until, from Late Pliocene to mid-Pleistocene times, soil-covered plains were transformed to stony deserts and, as aridity deepened, playas and extensive dunefields came into being. Thus, we suggest that the convex-up spurs, widespread throughout the MacDonnell Ranges and still soil-mantled today at Tyler Pass, evolved under soil cover that was lost as regional aridity deepened, perhaps in early or mid-Pleistocene times.

Conclusions

We examined a wide range of moderate to steep upland landscapes across Australia to quantify erosion rates and processes and to evaluate their dependence on climate. At first order, the slopes are either bedrock-dominated, weathering-limited surfaces or soil-mantled, transport-limited surfaces. We found robust support for the exponential decline of soil production rates with increasing soil thickness across the passive margin exposed in the Bega Valley in the humid SE. A soil-mantled site within the Arnhem escarpment in tropical monsoonal northern Australia showed a similar relationship with similar rates of soil production, except that the rate apparently declines at minimal soil thickness, suggesting a 'humped' soil production function (Heimsath *et al.* 2009).

Results from bedrock-dominated landscapes in semi-arid central Australia, mostly in hard sandstone, and a soil-mantled area at Tyler Pass, include very low erosion rates of less than 2 m Ma^{-1} on long, steep slopes at Mt Sonder and Kings Canyon, but range to *c*. 7 m Ma^{-1} on both bedrock spurs at Glen Helen and soil-mantled spurs at Tyler Pass. Comparable results were obtained from steep, rocky slopes in the semi-arid Flinders Ranges in southern Australia. Such slow rates of erosion suggest that the ridge–valley topography observed today was probably shaped under dramatically different climatic conditions, potentially during the late Miocene or early Pliocene.

The suite of results from different field sites indicates that erosion rates generally increase with increasing precipitation and decreasing temperature. However, to more completely quantify the potential relationship between erosion and climate we must include chemical weathering processes and a more rigorous quantification of palaeoclimates across the field sites. This compilation of results across Australia also emphasizes the robustness of cosmogenic nuclides to quantify millennial-scale erosion rates. Although these rates, and the different processes quantified across such different landscapes, offer a striking comparison of undisturbed landscapes, they do not capture the impact of recent anthropogenic land use. The rates do, however, provide critical parameters to help drive landscape evolution models seeking to explain the long-term evolution of the Earth's surface.

Cosmogenic nuclide measurements and field support were funded by The Research School of Earth Sciences (ANU), the US National Science Foundation (NSF) with post-doctoral support and grants DEB-0128995 and EAR-0239655 to A.M.H. Results from Arnhem Land were generated with D. Fink at the Australian Nuclear Science and Technology Organisation (ANSTO) and G. Hancock at the Department of Civil, Surveying and Environmental

Engineering, University of Newcastle. S. Selkirk used her magic wand to turn illegible 'blue line' 1:100 000 maps into the field maps for the MacDonnell Ranges field sites, and M. Zoldak made the regional topographic map. P. Bishop and an anonymous reviewer helped improve the manuscript with their comments.

References

Bagas, L. 1988. *Geology of Kings Canyon National Park*. Northern Territory Department of Mines and Energy, Report, **4**.

Belton, D. X., Brown, R. W., Kohn, B. P., Fink, D. & Farley, K. A. 2004. Quantitative resolution of the debate over antiquity of the central Australian landscape: implications for the tectonic and geomorphic stability of cratonic interiors. *Earth and Planetary Science Letters*, **219**, 21–34.

Bierman, P. R. 1994. Using *in situ* produced cosmogenic isotopes to estimate rates of landscape evolution; a review from the geomorphic perspective. *Journal of Geophysical Research, B, Solid Earth and Planets*, **99**, 13 885–13 896.

Bierman, P. R. & Caffee, M. 2002. Cosmogenic exposure and erosion history of Australian bedrock landforms. *Geological Society of America Bulletin*, **114**, 787–803.

Bierman, P. & Steig, E. J. 1996. Estimating rates of denudation using cosmogenic isotope abundances in sediment. *Earth Surface Processes and Landforms*, **21**, 125–139.

Braun, J., Heimsath, A. M. & Chappell, J. 2001. Sediment transport mechanisms on soil-mantled hillslopes. *Geology*, **29**, 683–686.

Burke, B. C., Heimsath, A. M., Chappell, J. & Yoo, K. 2009. Weathering the escarpment: chemical and physical rates and processes, southeastern Australia. *Earth Surface Processes and Landforms*, doi: 10.1002/esp.1764.

Cockburn, H. A. P. & Summerfield, M. A. 2004. Geomorphological applications of cosmogenic isotope analysis. *Progress in Physical Geography*, **28**, 1–42.

Dietrich, W. E., Reiss, R., Hsu, M.-L. & Montgomery, D. R. 1995. A process-based model for colluvial soil depth and shallow landsliding using digital elevation data. *Hydrological Processes*, **9**, 383–400.

Fujioka, T. & Chappell, J. 2010. History of Australian aridity: chronology in the evolution of arid landscapes. *In*: Bishop, P. & Pillans, B. (eds) *Australian Landscapes*. Geological Society, London, Special Publications, **346**, 121–139.

Gosse, J. C. & Phillips, F. M. 2001. Terrestrial *in situ* cosmogenic nuclides: theory and application. *Quaternary Science Reviews*, **20**, 1475–1560.

Granger, D. E., Kirchner, J. W. & Finkel, R. 1996. Spatially averaged long-term erosion rates measured from *in situ*-produced cosmogenic nuclides in alluvial sediment. *Journal of Geology*, **104**, 249–257.

Hancock, G. R. & Evans, K. G. 2006. Gully position, characteristics and geomorphic thresholds in an undisturbed catchment in northern Australia. *Hydrological Processes*, **20**, 2935–2951.

Hancock, G. R., Willgoose, G. R., Evans, K. G., Moliere, D. R. & Saynor, M. J. 2000. Medium term erosion simulation of an abandoned mine site using the SIBERIA landscape evolution model. *Australian Journal of Soil Research*, **38**, 249–263.

Hancock, G. R., Loughran, R. J., Evans, K. G. & Balog, R. M. 2008*a*. Estimation of soil erosion using field and modelling approaches in an undisturbed Arnhem Land catchment, Northern Territory, Australia. *Geographical Research*, **46**, 333–349.

Hancock, G. R., Lowry, J. B. C., Moliere, D. R. & Evans, K. G. 2008*b*. An evaluation of an enhanced soil erosion and landscape evolution model: a case study assessment of the former Nabarlek uranium mine, Northern Territory, Australia. *Earth Surface Processes and Landforms*, **33**, 2045–2063.

Hayes, D. E. & Ringis, J. 1973. Seafloor spreading in the Tasman Sea. *Nature*, **243**, 454–458.

Heimsath, A. M., Dietrich, W. E., Nishiizumi, K. & Finkel, R. C. 1997. The soil production function and landscape equilibrium. *Nature*, **388**, 358–361.

Heimsath, A. M., Dietrich, W. E., Nishiizumi, K. & Finkel, R. C. 1999. Cosmogenic nuclides, topography, and the spatial variation of soil depth. *Geomorphology*, **27**, 151–172.

Heimsath, A. M., Chappell, J., Dietrich, W. E., Nishiizumi, K. & Finkel, R. C. 2000. Soil production on a retreating escarpment in southeastern Australia. *Geology*, **28**, 787–790.

Heimsath, A. M., Chappell, J., Dietrich, W. E., Nishiizumi, K. & Finkel, R. C. 2001*a*. Late Quaternary erosion in southeastern Australia: a field example using cosmogenic nuclides. *Quaternary International*, **83–85**, 169–185.

Heimsath, A. M., Dietrich, W. E., Nishiizumi, K. & Finkel, R. C. 2001*b*. Stochastic processes of soil production and transport: erosion rates, topographic variation, and cosmogenic nuclides in the Oregon Coast Range. *Earth Surface Processes and Landforms*, **26**, 531–552.

Heimsath, A. M., Chappell, J., Spooner, N. A. & Questiaux, D. G. 2002. Creeping soil. *Geology*, **30**, 111–114.

Heimsath, A. M., Furbish, D. J. & Dietrich, W. E. 2005. The illusion of diffusion: field evidence for depth-dependent sediment transport. *Geology*, **33**, 949–952.

Heimsath, A. M., Chappell, J., Finkel, R. C., Fifield, L. K. & Alimanovic, A. 2006. Escarpment erosion and landscape evolution in southeastern Australia. *In*: Willett, S. D., Hovius, N., Brandon, M. T. & Fisher, D. M. (eds) *Tectonics, Climate and Landscape Evolution*. Geological Society of America, Special Papers, **398**, 173–190, doi: 10.1130/2006.2398(10).

Heimsath, A. M., Fink, D. & Hancock, G. R. 2009. The 'humped' soil production function: eroding Arnhem Land, Australia. *Earth Surface Processes and Landforms*, doi: 10.1002/esp.1859.

Kaste, J., Heimsath, A. M. & Bostick, B. C. 2007. Short-term soil mixing quantified with fallout radionuclides. *Geology*, **35**, 243–246.

Kohn, B. P., Gleadow, A. J. W., Brown, R. W., Gallagher, K., O'Sullivan, P. B. & Foster, D. A.

2002. Shaping the Australian crust over the last 300 million years: insights from fission track thermotectonic imaging and denudation studies of key terranes. *Australian Journal of Earth Sciences*, **49**, 697–717.

LAL, D. 1991. Cosmic ray labeling of erosion surfaces: *in situ* nuclide production rates and erosion models. *Earth and Planetary Science Letters*, **104**, 424–439.

LAMBECK, K. & STEPHENSON, R. 1985. Post-orogenic evolution of a mountain range; south-eastern Australian highlands. *Geophysical Research Letters*, **12**, 801–804.

NISHIIZUMI, K., KOHL, C. P. *ET AL.* 1993. Role of *in situ* cosmogenic nuclides ^{10}Be and ^{26}Al in the study of diverse geomorphic processes. *Earth Surface Processes and Landforms*, **18**, 407–425.

PERSANO, C., STUART, F. M., BISHOP, P. & BARFOD, D. N. 2002. Apatite (U–Th)/He age constraints on the development of the great escarpment on the southeastern Australian passive margin. *Earth and Planetary Science Letters*, **200**, 79–90.

PERSANO, C., STUART, F. M., BISHOP, P. & DEMPSTER, T. J. 2005. Deciphering continental breakup in eastern Australia using low-temperature thermochronometers. *Journal of Geophysical Research*, **110**, B12405, doi: 10.1029/2004JB003325.

PILLANS, B. 2007. Pre-Quaternary landscape inheritance in Australia. *Journal of Quaternary Science*, **22**, 439–447.

QUIGLEY, M., SANDIFORD, M., FIFIELD, K. & ALIMANOVIC, A. 2007*a*. Bedrock erosion and relief production in the northern Flinders Ranges, Australia. *Earth Surface Processes and Landforms*, **32**, 929–944.

QUIGLEY, M., SANDIFORD, M., FIFIELD, K. & ALIMANOVIC, A. 2007*b*. Landscape responses to intraplate tectonism: quantitative constraints from ^{10}Be nuclide abundances. *Earth and Planetary Science Letters*, **261**, 120–133.

REINHARDT, L. J., HOEY, T. B., BARROWS, T. T., DEMPSTER, T. J., BISHOP, P. & FIFIELD, L. K. 2007. Interpreting erosion rates from cosmogenic radionuclide concentrations measured in rapidly eroding terrain. *Earth Surface Processes and Landforms*, **32**, 390–406.

RICHARDSON, S. J. 1976. *Geology of the Michelago 1:100 000 sheet 8726*. Geological Survey of New South Wales, Department of Mineral Resources and Development, Canberra.

RILEY, S. J. & WILLIAMS, D. K. 1991. Thresholds of gullying, Arnhem Land, Northern Territory. *Malaysian Journal of Tropical Agriculture*, **22**, 133–143.

ROERING, J. J., KIRCHNER, J. W. & DIETRICH, W. E. 2001. Hillslope evolution by nonlinear, slope-dependent transport: steady state morphology and equilibrium adjustment timescales. *Journal of Geophysical Research—Solid Earth*, **106**, 16 499–16 513.

SAYNOR, M. J., ERSKINE, W. D., EVANS, K. G. & ELIOT, I. 2004. Gully initiation and implications for management of scour holes in the vicinity of Jabiluka mine, Northern Territory, Australia. *Geografiska Annaler Series A—Physical Geography*, **86**, 191–203.

SAYNOR, M. J., STABEN, G. *ET AL.* 2009. *Impact of Cyclone Monica on catchments within the Alligator Rivers Region. Field Survey Data*. Supervising Scientist, Darwin, Internal Report, **557**.

STABEN, G. & EVANS, K. G. 2008. Estimates of tree canopy loss as a result of Cyclone Monica, in the Magela Creek catchment, northern Australia. *Austral Ecology*, **33**, 562–569.

STEWART, A. J., BLAKE, D. H. & OLLIER, C. D. 1986. Cambrian river terraces and ridgetops in central Australia: oldest peristing landforms? *Science*, **233**, 758–761.

TOWNSEND, S. A. & DOUGLAS, D. D. 2000. The effect of three fire regimes on stream water quality, water yield and export coefficients in a tropical savanna (northern Australia). *Journal of Hydrology*, **229**, 118–137.

VASCONCELOS, P. M., KNESEL, K. M., COHEN, B. E. & HEIM, J. A. 2008. Geochronology of the Australian Cenozoic: a history of tectonic and igneous activity, weathering, erosion, and sedimentation. *Australian Journal of Earth Sciences*, **55**, 865–914.

WEISSEL, J. K. & SEIDL, M. A. 1997. Influence of rock strength properties on escarpment retreat across passive continental margins. *Geology*, **25**, 631–634.

WEISSEL, J. K. & SEIDL, M. A. 1998. Inland propagation of erosional escarpments and river profile evolution across the southeast Australian passive continental margin. *In*: TINKLER, K. J. & WOHL, E. E. (eds) *Rivers Over Rock: Fluvial Processes in Bedrock Channels*. Geophysical Monograph, American Geophysical Union, **107**, 189–206.

WELLS, T., WILLGOOSE, G. R. & HANCOCK, G. R. 2008. Modeling weathering pathways and processes of the fragmentation of salt weathered quartz–chlorite schist. *Journal of Geophysical Research—Earth Surface*, **113**, F01014, doi: 10.1029/2006JF000714.

WILKINSON, M. T., CHAPPELL, J., HUMPHREYS, G. S., FIFIELD, K., SMITH, B. & HESSE, P. 2005. Soil production in heath and forest, Blue Mountains, Australia: influence of lithology and palaeoclimate. *Earth Surface Processes and Landforms*, **30**, 923–934.

WILLIAMS, M., PRESCOTT, J., CHAPPELL, J., ADAMSON, D., COCK, B., WALKER, K. & GELL, P. 2001. The enigma of a late Pleistocene wetland in the Flinders Ranges, South Australia. *Quaternary International*, **83–85**, 129–144.